JOURNAL OF BONE AND MINERAL RESEARCH
Volume 24, Number 11, 2009
Published online on May 4, 2009; doi: 10.1359/JBMR.090502

Dose-Dependent Effects of *Runx2* on Bone Development

Shiqin Zhang,[1,2] Zhousheng Xiao,[1,2] Junming Luo,[1] Nan He,[1] Josh Mahlios,[1] and L. Darryl Quarles[1]

ABSTRACT: Runx2 controls the commitment of mesenchymal cells to the osteoblastic lineage. Distinct promoters, designated P1 and P2, give rise to functionally similar *Runx2*-II and *Runx2*-I isoforms. We postulate that this dual promoter gene structure permits temporal and spatial adjustments in the amount of *Runx2* isoforms necessary for optimal bone development. To evaluate the gene dose–dependent effect of *Runx2* isoforms on bone development, we intercrossed selective Runx2-II$^{+/-}$ with nonselective Runx2-II$^{+/-}$/Runx2-I$^{+/-}$ mice to create compound mutant mice: Runx2-II$^{+/-}$, Runx2-II$^{+/-}$/Runx2-I$^{+/-}$, Runx2-II$^{-/-}$, Runx2-II$^{-/-}$/Runx2-I$^{+/-}$, Runx2-II$^{-/-}$/Runx2-I$^{-/-}$. Analysis of the different Runx2-deficient genotypes showed gene dose–dependent differences in the level of expression of the *Runx2* isoforms. In addition, we found that Runx2-I is predominately expressed in the perichondrium and proliferating chondrocytes, whereas *Runx2*-II is expressed in hypertrophic chondrocytes and metaphyseal osteoblasts. Newborn mice showed impaired development of a mineralized skeleton, bone length, and widening of the hypertrophic zone that were proportionate to the reduction in total Runx2 protein expression. Osteoblast differentiation ex vivo was also proportionate to total amount of Runx2 expression that correlated with reduced Runx2 binding to the osteocalcin promoter by quantitative chromatin immunoprecipitation analysis. Functional analysis of P1 and P2 promoters showed differential regulation of the two promoters in osteoblastic cell lines. These findings support the possibility that the total amount of Runx2 derived from two isoforms and the P1 and P2 promoters, by regulating the time, place, and amount of Runx2 in response to changing environmental cues, impacts on bone development.
J Bone Miner Res 2009;24:1889–1904. Published online on May 4, 2009; doi: 10.1359/JBMR.090502

Key words: *Runx*2 isoforms, knockout mouse, gene dosage, embryonic bone development, osteoblast differentiation

Address correspondence to: *L. Darryl Quarles, MD, University of Kansas Medical Center, MS 3018, 3901 Rainbow Boulevard, 6018 Wahl Hall East, Kansas City, KS 66160, USA, E-mail: dquarles@kumc.edu*

INTRODUCTION

RUNX2 IS A MASTER transcription factor regulating both embryonic bone development and postnatal osteoblastic function.[1] The disruption of *Runx2* function in mice and hereditary skeletal disorders caused by inactivating *Runx2* mutations establishes the essential and nonredundant role of *Runx2* in osteoblast and terminal chondrocyte differentiation.[2–6] *Runx2* transcriptional activation requires binding to the ubiquitously expressed Cbfβ transcriptional co-activator and the presence of consensus *cis*-acting sequence PuACCPuCA in the promoters of target genes.[7] Runx2 expression and function are regulated at multiple levels, including two promoters, P1 and P2, that transcribe two major isoforms, designated *Runx2*-II and *Runx2*-I, which differ only in their respective N termini (MASNS for Runx2-II and MRIPV for Runx2-I),[8–10] a complex 5′UTR that may regulate message stability and other functional domains permitting post-translational modifications (phosphorylation, ubiquitination) of Runx2 in response to growth factor signaling (e.g., mitogen activated protein kinase [MAPK], fibroblast growth factor [FGF], PTH/PTH-related peptide [PTHrP]).[11,12] *Runx2* also integrates many developmental and growth factor signals through the presence of a myriad of structural domains that act as scaffolds for stimulatory and inhibitory co-regulatory proteins.[8,13–23]

It is becoming apparent that these complex control mechanisms regulating the amount and location of Runx2 expression are critical to this transcription factor's functions. Whereas increments in Runx2 expression stimulate mesenchymal cells to differentiate into osteoblasts but inhibit their differentiation into chondrocytes and adipocytes,[24] Runx2 must be suppressed for immature osteoblasts to become fully mature,[24] and the ectopic expression of Runx2 is associated with malignancies.[25] Differential promoter utilization is important in determining the location of Runx2 isoform expression and their differences on bone development in vivo. In this regard, selective Runx2-II$^{-/-}$ mice have a predominant impairment of endochondral bone formation, whereas *Runx2*-I seems to function to regulate early osteoblastogenesis and the formation of cortical and intramembranous bone.[26,27]

Dr. Quarles serves as a Consultant for Amgen, Cytochroma, and GlaxoSmithKline and has grants from Servier. All other authors state that they have no conflicts of interest.

[1]The Kidney Institute, University of Kansas Medical Center, Kansas City, Kansas, USA; [2]These authors contributed equally to this study.

Except for increased potency of Runx2-II in vitro, however, Runx2-I and Runx2-II isoforms have nearly identical functions.[15,27–30] Moreover, Runx2-I and Runx2-II, as well as Runx paralogs, can substitute for one another in vitro and in vivo.[27,28,30–33] It is unclear why there is a need for a complex dual promoter gene structure to generate separate gene products of similar function.

One possibility is that a critical dose of Runx2, at a particular time and place, under the control of the P1 and P2 promoter, is critical for normal bone development and postnatal osteoblast function. To date, insights into the possibility that Runx2 exerts important gene dose effects on skeletal development have been derived from observations that heterozygous nonselective *Runx2*– and selective *Runx2*-II–deficient mice have less severe bone abnormalities than homozygous mice[2,3] and from transgenic mice overexpression of Runx2 paradoxically showing impaired osteoblastic function and increased bone resorption.[34,35] Recently, study of a hypomorphic *Runx2* mutant allele indicates that there is a minimal requirement of ~80% functional Runx2 for normal bone development in mice.[36] It has been challenging to develop a selective *Runx2*-I knockout mouse model to separately assess the contribution of the Runx2-I isoform and separately assess the graded effects of loss of the Runx2-I and Runx2-II isoforms below the threshold for normal skeletal development. In this study, transferred nonselective *Runx2*– and selective *Runx2*-II–deficient mice onto a C57BL/6J background and intercrossed these mice in various combinations to generate compound mutant mice with graded reductions in the levels of Runx2-I and II isoform expression. Using this model, we examined the hypothesis that the amount of total Runx2 expression, controlled by the composite of Runx2-I and Runx2-II expression from their respective P2 and P1 promoters, is predominantly responsible for the apparent differential effects of *Runx2* isoforms on intramembranous and endochondral bone formation. We show that there is a critical gene dose requirement for Runx2 for skeletal development.

MATERIALS AND METHODS

Animals

Selective *Runx2*-II–deficient mice (Runx2-II$^{+/-}$) were generated in our laboratory as previously described,[27] and nonselective *Runx2* mutant mice (Runx2-II$^{+/-}$/Runx2-I$^{+/-}$) were obtained from Dr. Gerard Karsenty.[3] In the selective *Runx2*-II mutant mice, both the proximal P1 promoter and exon 1 are deleted.[27] In the nonselective *Runx2* mutant mice, *Runx2* expression is disrupted by the insertion of an IRES-*LacZ*-pA and MC1-*Neo*-pA cassette in exon 2.[3] All mice were bred and maintained on a C57BL/6J background. We used three different breeding strategies. Selective *Runx2*-II heterozygous (Runx2-II$^{+/-}$)– and homozygous (Runx2-II$^{-/-}$)–deficient mice were generated by mating male and female selective *Runx2*-II heterozygous mice. Nonselective *Runx2*-II heterozygous (Runx2-II$^{+/-}$/Runx2-I$^{+/-}$)– and homozygous (Runx2-II$^{-/-}$/Runx2-I$^{-/-}$)–deficient mice were generated by mating male and female nonselective *Runx2*-II heterozygous mice. Compound heterozygous Runx2-II$^{+/-}$ and Runx2-II$^{+/-}$/Runx2-I$^{+/-}$ mice (Runx2-II$^{-/-}$/Runx2-I$^{+/-}$) were generated by intercrossing our selective *Runx2*-II heterozygous mice with the nonselective *Runx2* heterozygous mice (Table 1).

TABLE 1. Genotype of Groups

Group	*Genotype*
Group 1	Wildtype
Group 2	Runx2-II$^{+/-}$ (lack one copy of *Runx2*-II)
Group 3	Runx2-II$^{+/-}$/Runx2-I$^{+/-}$ (lack one copy of *Runx2*-II and *Runx2*-I)
Group 4	Runx2-II$^{-/-}$ (lack both copies of *Runx2*-II)
Group 5	Runx2-II$^{-/-}$/Runx2-I$^{+/-}$ (lack one copy of *Runx2*-I and two copies of *Runx2*-II)
Group 6	Runx2-II$^{-/-}$/Runx2-I$^{-/-}$ (lack two copies of *Runx2*-II and *Runx2*-I)

In situ hybridization, microdissection, and RT-PCR analysis

The *Runx2*-II, *Runx2*-I isoform-specific, type X collagen, and *osteopontin* cDNA probes were linearized with restriction enzyme and purified using a QIAquick gel extraction kit (QIAGEN, Valencia, CA, USA) as previously described.[37] The antisense and sense cRNA probes were synthesized, labeled, and purified following the protocol of a T3/T7 or SP6 Digoxin RNA probes labeling kit (Roche Applied Science, Indianapolis, IN, USA). For in situ hybridization, 5-μm sections of bone tissues were cut and placed on the positively charged glass slides. The sections were deparaffinized and rehydrated to PBS with Tween 20 (PBST) and fixed with fresh prepared cold 4% paraformaldehyde solution (PFA) followed by proteinase K digestion and 4% PFA refixation and acetylation. The slides were incubated with 1.0 μg/ml antisense or sense probes at 56°C overnight. After hybridization, the slides were washed, blocked, and incubated with a 1:5000 alkaline phosphatase anti-Digoxin Fab fragment at 4°C overnight. The color development was carried with a Vector Red Alkaline Phosphatase Substrate kit (Vector Laboratories, Burlingame, CA, USA), and the sections were counterstained with Vector Methyl Green (Vector Laboratories).

For laser capture microdissection (LCM), the hindlimbs of E17.5 mice were removed and embedded in O.C.T. Compound (Tissue-Tek; Fisher Scientific, Pittsburgh, PA, USA). Longitudinal sections (10 μm) were cut and put on membrane slides (Leica Microsystems, Bannockburn, IL, USA). The sections were immediately stained using a LCM crystal violet staining kit (Ambion, Austin, TX, USA), and the hypertrophic zone, trabecular bone, bone collar, proliferation zone, and perichondrium were selectively dissected under a laser capture microscope. The total RNA from these microdissections was isolated using an RNeasy Micro Kit (QIAGEN) according to manufacturer's protocol. RT-PCR was carried out with either *Runx2* isoform-specific or type X collagen primers using the Titan One

tube RT-PCR kit (Roche Applied Science) as previously described,[8,38] and mouse cyclophilin A was amplified as a control for the RT-PCR reactions.

Immunohistochemistry

The E17.5 embryos were fixed in 4% PBS-buffered formalin overnight and decalcified in 15% EDTA-PBS for 2 wk. The hindlimbs of embryos were removed and processed for paraffin embedding. Five-micrometer sections of bone tissues were put on the positively charged glass slides (Superfrost Plus; Fisher Scientific). Immunohistochemistry was carried out using M.O.M Kits (Vector Laboratories, Youngstown, OH, USA). Briefly, the slides were deparaffinized and rehydrated to PBST buffer. Antigen unmasking was achieved using 0.01 M citrate buffer (pH 6.0) to boil for 20 min. Endogenous peroxidase was blocked by treating the slides with 3% hydrogen peroxide in water for 5 min. Avidin/biotin blocking was performed using a Vector Avidin/biotin blocking kit (Vector Laboratories). The mouse IgG blocking process was carried out with 1-h incubation of mouse IgG blocking reagent. The slides were incubated with Runx2 monoclonal antibody (1:100; MBL International, Woburn, MA, USA) at room temperature for 30 min. The negative control sections were incubated with 0.01 M 1× PBS. Thereafter, the slides were treated with ready-to-use biotinylated secondary antibody and VECTSTAIN Elite ABC reagent (Vector Laboratories), followed by standardized development using a Vector NovaRed substrate kit (Vector Laboratories), and the sections were counterstained with Vector Methyl Green (Vector Laboratories).

Whole skeletal mount Alizarin red/Alcian blue staining and histological preparations

Whole mouse carcasses were collected from newborn mice after death, defatted for 2–3 days in acetone, stained sequentially with Alcian blue and Alizarin red S in 2% KOH, cleared with 1% KOH/20% glycerol, and stored in 50% ETOH/50% glycerol. Femurs and tibias from newborn mice were decalcified at 4°C in 12.5% EDTA/2.5% paraformaldehyde in PBS. Longitudinal sections were stained with H&E to assess the histology of the growth plate in femurs and tibias.[27,39] The hypertrophic zone was defined by visual inspection of enlarging cell size in the zone on the histology slide and by expression of type X collagen mRNA through in situ hybridization analysis. The length of the entire tibias, formation of bone marrow cavity, and hypertrophic zone of growth plate were calculated using NIH (Bethesda, MD, USA) Image J software (V1.33m) as previously described.[40,41]

μCT analysis

For newborn mice, the whole mouse skeleton and full-length tibias were scanned using a μCT 40 in high resolution (Scanco Medical, Southeastern, PA, USA). The length of mineralized tibias was calculated using the number of scanned slices. 3D images and longitudinal sections of mineralized tibias were generated using the following values for a gauss filter (sigma 0.8, support 1) and a threshold of 200. One hundred slices of the metaphyses under the growth plate, constituting 0.6 mm in length, and 50 slices of the diaphysis, constituting 0.3 mm in length, were selected. 3D image analysis was performed to determine bone volume (BV/TV) and cortical thickness (Ct.Th) as previously described.[27]

Real-time RT-PCR

For quantitative real-time RT−PCR, 2.0 μg total RNA isolated from E17.5 embryos was reverse transcribed as previously described.[8] PCR reactions contained 100 ηg template (cDNA or RNA), 300 ηM each forward and reverse primer, and 1× iQ SYBR Green Supermix (Bio-Rad, Hercules, CA, USA) in 50 μl. Samples were amplified for 40 cycles in an iCycler iQ Real-Time PCR Detection System with an initial melt at 95°C for 10 min, followed by 40 cycles of 95°C for 15 s and 60°C for 1 min. PCR product accumulation was monitored at multiple points during each cycle by measuring the increase in fluorescence caused by the binding of SybrGreen I to dsDNA. The threshold cycle (Ct) of tested-gene product from the indicated genotype was normalized to the Ct for cyclophilin A.

Western blot analysis, alkaline phosphatase activity, and mineralization assays in immortalized osteoblast cultures

Calvaria from E17.5 embryos were used for the isolation of osteoblasts by sequential collagenase digestion as previously described.[27,42] To engineer immortal osteoblast cell lines, isolated primary osteoblasts were infected using a retroviral vector carrying SV40 large and small T antigen as previously described.[27,42] Briefly, cells were grown in 100-mm plates at ~50–60% confluent the day before infection. On the day of infection, the medium was removed and replaced with a medium containing SV40 large and small T antigen-helper-free viral supernatant in the presence of 4 μg/ml of polybrene (Sigma, St. Louis, MO, USA) for 48 h. The cells were allowed to recover for 72 h followed by selection with 1 μg/ml puromycin (Sigma) for 3–4 days. The immortalized osteoblasts were characterized following the protocols below.

For Western blot analysis, nuclear extracts from cultured osteoblasts were prepared using a NE-PER nuclear extraction kit (Pierce Chemical, Rockford, IL, USA). Protein concentrations were determined with a Bio-Rad protein assay kit (Bio-Rad). Equal quantities of protein were subjected to NuPAGE 4–12% Bis-Tris Gel (Invitrogen, Carlsbad, CA, USA) and analyzed with standard Western blot protocol.[8,39] Primary Runx2 monoclonal antibody was obtained from MBL International (Woburn, MA, USA), and lamin A/C antibody was purchased from Santa Cruz Biotechnology (Santa Cruz, CA, USA). Signals were detected using horseradish peroxidase–conjugated secondary antibodies (Santa Cruz Biotechnology) and an enhanced chemiluminescence detection kit (ECL Plus Western Blotting Detection Reagents; GE Healthcare, Piscataway, NJ, USA).

To induce differentiation, the immortalized osteoblasts were plated at a density of 1×10^5 cells per well in a 6-well plate and grown for period of up to 14 days in αMEM containing 10% FBS supplemented with 5 mM β-glycerophophate (β-GP) and 25 μg/ml of ascorbic acid (AA). Alkaline phosphatase activity and Alizarin red-S histochemical staining for mineralization were performed as previously described.[27] Total DNA content was measured with a PicoGreen dsDNA quantification reagent and kit (Molecular Probes, Eugene, OR, USA).

Quantitative chromatin immunoprecipitation analyses

The quantitative chromatin immunoprecipitation (qChIP) analyses were performed using the ChIP-IT kit (Active Motif, Carlsbad CA) and modifications of previously described methods.[43] Briefly, immortalized osteoblasts were cultured in differentiation medium (containing 5 mM β-GP and 25 μg/ml of AA) for 6 days and treated with 1% formaldehyde to cross-link chromatin. Immunoprecipitation was performed using anti-Runx2 antibody (M-70; sc10758; Santa Cruz Biotechnology) and protein A agarose. The specific protein–DNA complex was reversely cross-linked, and DNA fragments were purified. Real-time PCR was performed using primers located in the OSE2a site of *osteocalcin* promoter as previously reported.[44] Primers amplifying exon 4 that does not contain any Runx2-binding sites were used to normalize for DNA content and to calculate the relative ratio of the OSE2a sequence over control sequence. Fold enrichment reflects the ratio of OSE2a/control sequence in the immunoprecipitation versus the input samples. Nonspecific normal rabbit IgG was used as a negative control.

Analysis of transcription factor binding sites in the P1 and P2 promoter of Runx2 gene

We used the *rVISTA* program to map the *cis*-regulatory elements in the 5.4-kb P1 and 12.0-kb P2 promoter of *Runx2* gene.[45,46] We also used PCR to subclone 2.0 kb of proximal P2 promoter [P2(2.0)-LUC] into pluc4 vector as we did on 1.4 kb of proximal P1 region [P1(1.4)-LUC] before.[47] The P1 and P2 promoter activities were assessed by measuring luciferase activity 48 h after transfection into ROS17/2.8 and MC3T3-E1 osteoblastic cell lines using the electroporation protocol from Amaxa's Biosystems as the manufacturer describes (Amaxa).[39] To study the effects of different osteogenic factors (such as TGF-β and Wnt3a) on P1 and P2 promoter activity, Ros17/2.8 cells were transiently co-transfected with either P1(1.4)-LUC or P2(2.0)-LUC along with *Renilla* luciferase-null (RL-null; Promega, Madison, WI, USA) as an internal control for 24 h, and the cells were starved in 0.1% serum medium for 24 h before stimulants were added. After treatment with 5%FBS growth medium in the presence or absence of osteogenic factors (such as TGF-β and Wnt3A) for 8 h, cell lysates were harvested, and luciferase activity was determined using the Dual-Luciferase reporter assay (Promega) and luminometer according to the manufacturer's specifications.[39] Wnt3a-containing conditioned medium (CM) was harvested from L Wnt-3A cells according to the protocol provided by the American Type Culture Collection (ATCC). The control CM was collected from control L cells. To examine the autoregulation of *Runx2* gene, we also transiently co-transfected P1(1.4)-LUC or P2(2.0)-LUC along with either *Runx2*-II or *Runx2*-I full-length cDNA expressing plasmids into MC3T3-E1 osteoblasts, respectively, and pcDNA3.1 vector alone was used for control as previously described.[28]

Statistics

We evaluated differences between groups by one-way ANOVA. All values are expressed as means ± SD. All computations were performed using the STATGRAPHICS statistical graphics system (STSC).

RESULTS

Spatial and temporal expression of P1- and P2-dependent Runx2-II and Runx2-I expression in bone

First, we performed in situ hybridization with either *Runx2*-I or *Runx2*-II isoform-specific antisense probes on embryonic tibias of wildtype mice to examine the effects of P1 and P2 promoters to regulate the spatial distributions of Runx2 isoforms. In E17.5 tibias from wildtype mice, we found the P2 promoter results in expression of *Runx2*-I predominantly in the perichondrium and periosteum, as well as proliferating and resting chondrocytes, but minimal expression in hypertrophic chondrocytes. In contrast, P1 promoter-mediated expression of *Runx2*-II occurs in the terminal hypertrophic zone, trabecular bone in the metaphysis, and periosteum, but not in the perichondrium, and the hypertrophic zone of growth plate was confirmed by using type X collagen riboprobe (Fig. 1A). Microdissection of mRNAs from these various regions followed by conventional RT-PCR using *Runx2*-II and *Runx2*-I as well as type X collagen–specific primers corroborated the in situ findings. This analysis showed that *Runx2*-II is not expressed in the perichondrium, whereas *Runx2*-I is not expressed in the hypertrophic zone (Fig. 1B). In contrast, type X collagen expression was only expressed in the hypertrophic zone (Fig. 1B). We also found that both *Runx2*-I and *Runx2*-II isoforms are highly expressed in calvarial bone and in MC3T3-E1 osteoblasts (Fig. 1B).

Next, to explore the temporal expression of *Runx2* isoforms during embryogenesis, we performed real-time RT-PCR analysis using mouse embryos RNAs from E11.5 to E17.5. We found that P2-dependent *Runx2*-I expression is upregulated between E11.5 and E13.5 and decreases between E13.5 and E17.5 (Fig. 1C). In contrast, P1-dependent *Runx2*-II expression is progressively upregulated throughout embryonic development, attaining a maximal 5-fold increase between E13.5 and E17.5 (Fig. 1D).

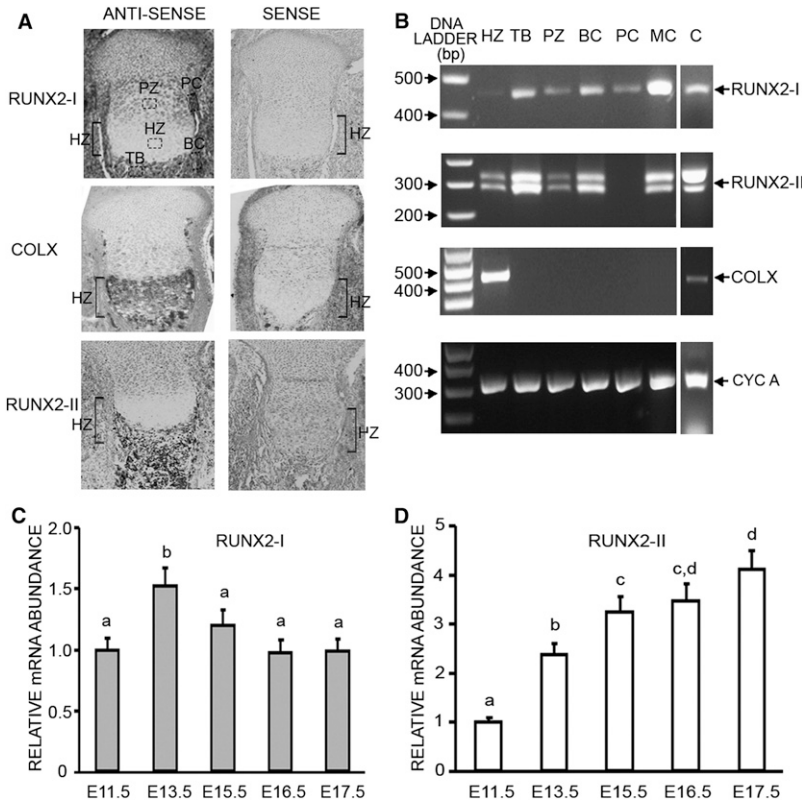

FIG. 1. Spatial and temporal expression of *Runx2* isoforms in embryonic bone. (A) In situ hybridization with respective *Runx2*-I– and *Runx2*-II–specific antisense riboprobes (indicated by red staining) showed predominant *Runx2*-I expression in the perchondrium and bone collar (left first panel) and *Runx2*-II in terminal hypertrophic zone and trabecular bone in the metaphysis (left third panel). *Type X collagen* (*COLX*) antisense riboprobe (indicated by black staining) showed *COLX* expression only in the hypertrophic zone of growth plate (left second panel). In contrast, the sense probes produced no labeling (right first, second, and third panels). (B) RT-PCR of microdissected RNA from different bone sites using laser capture showed that *Runx2*-I is highly expressed in the trabecular bone (TB) and bone collar (BC), but weakly expressed in cartilage, including the hypertrophic zone (HZ) (first panel). In contrast, *Runx2*-II expression is also widely distributed but is absent in the perichondrium (second panel). Again, type X collagen expression was only expressed in the hypertrophic zone (third panel). In addition, both *Runx2* isoforms but not *COLX* is expressed in calvarial bone (C) and MC3T3-E1 osteoblasts (MC). Cyclophilin A (*CYC A*) was used an internal control (bottom panel). HZ, hypertrophic zone; TB, trabecular bone; PZ, proliferation zone; BC, bone collar; PC, perichondrium; MC, MC3T3-E1; C, calvaria. (C and D) Temporal expression of Runx2 isoforms in wildtype whole embryos by real-time RT-PCR analysis. *Runx2*-I (C) is transiently upregulated between E11.5 and E13.5 (~1.5-fold), and remains constant between E13.5 and E17.5. In contrast, *Runx2*-II (D) is progressively upregulated throughout embryonic development, reaching a maximum of 5-fold elevation between E13.5 and E 17.5. Data are expressed as the fold changes relative to the housekeeping gene *Cyclophilin A* and represent the mean ± SD from three to four individual samples at the indicated days of mouse gestation from E11.5 to E17.5. Values sharing the same superscript are not significantly different at $p < 0.05$.

Compound selective Runx2-II– and nonselective Runx2–deficient mice show gene dose–dependent effects of p2Runx2-I and p1Runx2-II on bone development

To study the role of *Runx2*-II and *Runx2*-I on bone development, we created compound selective *Runx2*-II– and nonselective *Runx2*–deficient mice by intercrossing selective *Runx2*-II heterozygous mice with the nonselective *Runx2* heterozygous mice. This breeding strategy resulted in six separate genotypes with different number of *Runx2* alleles (Table 1). These include group 1 (wildtype), group 2 (Runx2-II$^{+/-}$, selective heterozygous Runx2-II$^{+/-}$ mice with loss of one copy of *Runx2*-II but retaining both copies of *Runx2*-I), group 3 (Runx2-II$^{+/-}$/Runx2-I$^{+/-}$, nonselective *Runx2* heterozygous mice that have loss of one copy each of the type I and II isoforms), group 4 (Runx2-II$^{-/-}$, lacks both copies of *Runx2*-II but retain both copies of *Runx2*-I), group 5 (Runx2-II$^{-/-}$/Runx2-I$^{+/-}$, double heterozygous selective *Runx2*-II and nonselective *Runx2* mice, which lack one copy of the type I and two copies of type II isoforms), and group 6 (Runx2-II$^{-/-}$/Runx2-I$^{-/-}$, nonselective *Runx2* homozygous mice, which lack all four alleles encoding both *Runx2*-I and II isoforms).

Mice were born at the expected Mendelian frequency. The gross survival of group 2 (single selective Runx2-II$^{+/-}$ mice) and group 3 (single nonselective Runx2-II$^{+/-}$/Runx2-I$^{+/-}$ mice) newborn mice was not different from wildtype littermates (group 1). In contrast, mice in groups 4–6 had perinatal lethality.

We observed a direct correlation between the genotype and amount of Runx2 protein expression (Fig. 2). Both immunostaining and Western blot analysis showed a progressive reduction in the total amount of Runx2 protein

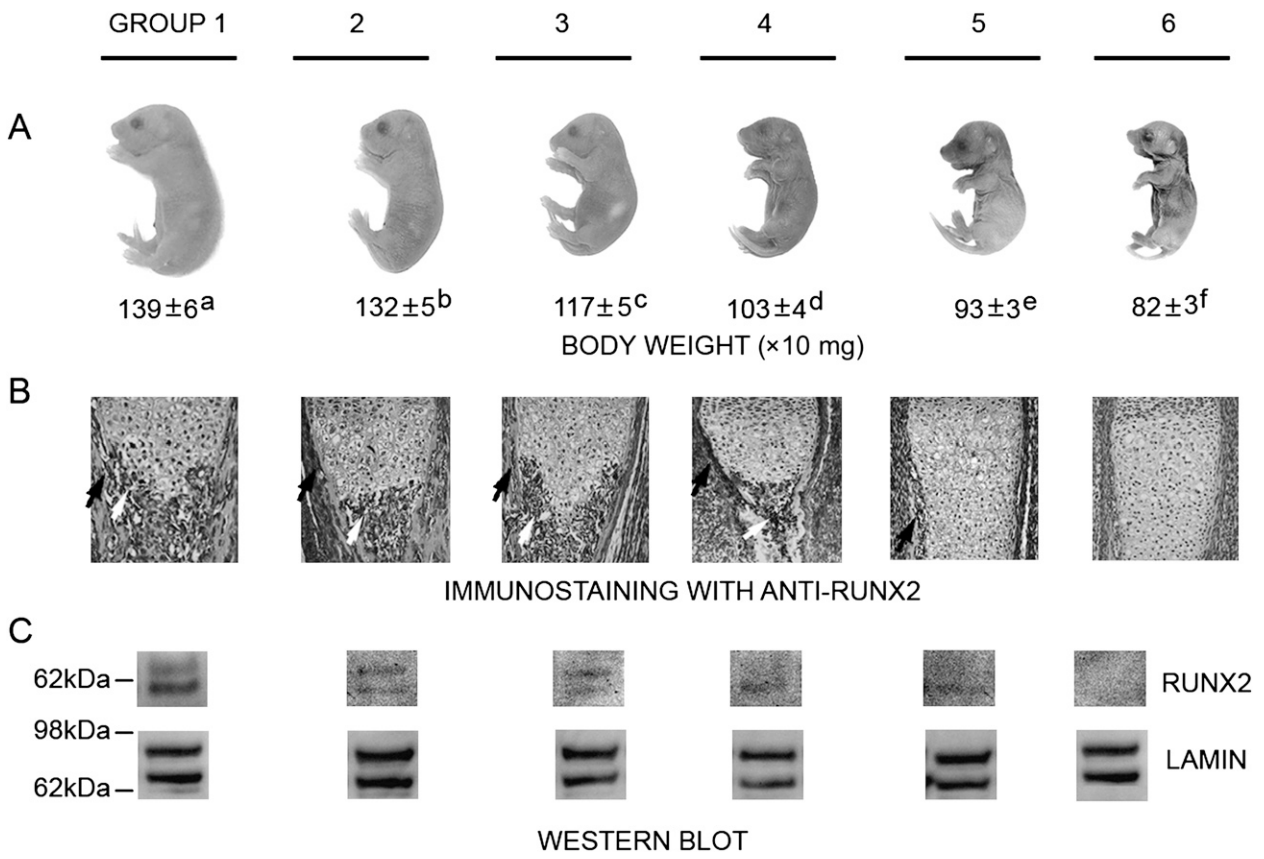

FIG. 2. Gross appearance, body weight, and Runx2 protein levels in compound Runx2-I and -II isoform-deficient mice. (A) Gross appearance and body weight in newborn wildtype and compound Runx2 isoform-deficient mice. Body weight (expressed in mg) represents mean ± SD from five to six mice. Values sharing the same superscript are not significantly different at $p < 0.05$. (B) Immunodetection of Runx2 expression in tibias from E17.5 mice. Immunostaining with anti-Runx2 antibody shows that Runx2 protein is differentially expressed in hypertrophic chondrocytes and osteoblasts in the metaphyseal region (white arrow) and in the perichondrium (yellow arrow) as a function of geneotype. Overall, the density of the nuclear staining was progressively decreased as a function of gene dose. Magnification (×100). (C) Western blot analysis of total Runx2 protein expression in calvarial osteoblasts. The top panel shows the 64- and 60-kDa bands, respectively, representing the full-length and alternatively spliced Runx2 protein.[85] The bottom panel shows the 70-kDa lamin A/C protein, which was used as a control for protein expression. The amount of Runx2 protein corresponds to the gene dose in the various genotypes.

expression in accordance with the graded deficiency of Runx2-I and Runx2-II alleles in groups 1–6 (Figs. 2B and 2C). Because the nonselective Runx2 mutant mice still generate nonfunctional *Runx2* mRNAs and have intact P1 and P2 promoter function, the levels of total Runx2 message expression did not correlate with the Runx2 protein levels in the various genotypes (data not shown).

There was a direct relationship between the amount of Runx2 expressed and observed skeletal abnormalities (Fig. 2A). In addition, the body weight of *Runx2*-deficient mice, which likely is an indirect marker of the underlying changes in skeletal development, decreased progressively from group 1 to group 6 mice (Fig. 2A). Specific abnormalities in the various groups are as follows.

Group 2 (Runx2-II$^{+/-}$) mice, representing the loss of one *Runx2*-II allele, had no apparent skeletal abnormalities by Alizarin red/Alcian blue skeletal staining (Fig. 3). Examination of E17.5 embryos from group 2 mice with the more sensitive μCT and bone histological analysis, however, showed a significant reduction in the length of mineralized tibia and trabecular bone volume in the metaphyseal region (Figs. 4 and 5), indicating that loss of a single copy of the *Runx*2-II isoform is sufficient to reduce endochondral bone formation.

Group 3 mice (loss of one copy each of *Runx*2-I and *Runx*2-II allele) had a more severe phenotype than group 2 mice. Group 3 mice (Runx2-II$^{+/-}$/Runx2-I$^{+/-}$) exhibited delayed ossification of cranial, nasal, clavicular, hyoid bone, pubic, and ischial bones (Fig. 3), similar to previous reports.[3] μCT analysis showed an ~10% and 44% reduction in the length of mineralized tibia and trabecular bone volume in the metaphyseal region in group 3 mice (Fig. 4), respectively. Bone histological analysis showed an increase in hypertrophic zone, decrease in length of entire tibia and bone marrow cavity formation, and trabecular bone formation and thinning of the cortex, reflecting abnormalities in both endochondral and intramembranous bone formation.

Group 4 (loss both copies of *Runx*2-II but retain both copies of *Runx*2-I) mice showed more severe abnormalities

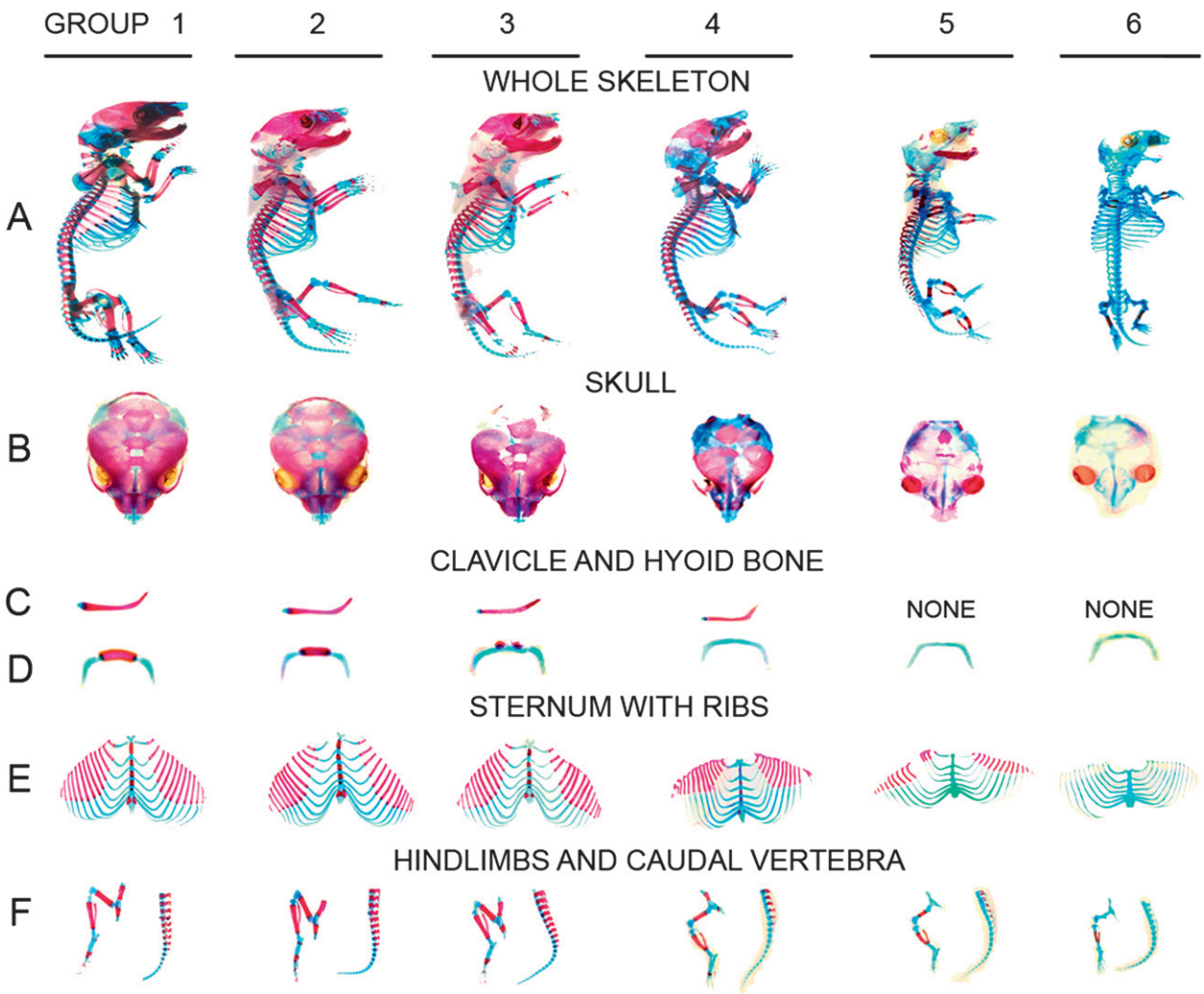

FIG. 3. Defective skeletogenesis in compound Runx2-I and -II isoform-deficient newborn mice. Alizarin red/Alcian blue staining of group 1 to group 6 newborn mice. Calcified tissues are stained red, and cartilage is stained blue. (A–F) Whole skeleton, a superior view of the skull, clavicles, hyoid bone, sternum and ribs, scapula, and forelimb (left image) and caudal vertebrae (right image), respectively. Arrows indicated delayed ossification of specific bones. Compared with the wildtype, there was a gene dose–dependent effect on skeletogenesis that included defects of both endochondral and intramembranous bone formation. Defects in skull and appendicular and axial skeleton were proportionate to the reduced gene dose in the various Runx2 genotypes. There is a progressive gene dose–dependent reduction of occipital bone, posterior zygomatic arches, and nasal bone of the skull (B). In addition, there was a gene dose–dependent defect in the distal clavicles in groups 2–4 and a total absence of the clavicle in groups 5 and 6 (C). Mineralization of the hyoid bone was absent in groups 4–6 (D). The distal ribs and sternum (E), as well as phalangeal bones and the caudal spine (F), showed a progressive delay in ossification that was proportionate to the reduction in gene dose.

of endochondral bone than intramembranous bone (Figs. 3–5), reflected by absent occipital bones, which are formed by endochondral bone formation, and posterior zygomatic arches, as well as impaired formation of nasal bones and abnormalities of the hyoid bone, distal clavicles, and distal ribs, shorter long bones, absent ossification centers in phalangeal bones with absent ossification centers, and delayed endochondral ossification of the caudal spine, similar to previous reports.[27] Cranial and cortical bones, which are derived from mesenchymal precursors, were present in group 4 (Runx2-II$^{-/-}$) mice. μCT analysis confirmed that the selective Runx2-II$^{-/-}$–null mice had a further reduction in length of mineralized tibia and exhibited predominant defects of endochondral bone but with relative preserved formation of intramembranous and cortical bone (Fig. 4). Histologically, the tibias from Runx2-II$^{-/-}$/Runx2-I$^{+/+}$ mice had a wider zone of hypertrophic chondrocytes, and the length of entire tibia, formation of bone marrow cavity, and the primary trabeculae in the metaphyseal region were markedly diminished compared with group 3 (Fig. 5).

Group 5 mice (the compound selective *Runx2*-II and nonselective *Runx2* heterozygous mice), which reflect the presence of one p2-*Runx2*-I allele (Runx2-II$^{-/-}$/Runx2-I$^{+/-}$), had a more severe phenotype than group 4 (Runx2-II$^{-/-}$) selective homozygous Runx2-II$^{-/-}$ mice. Group 5 mice formed partial axial and appendicular bone and proximal ribs and mandibles, but lacked calvaria and clavicles in

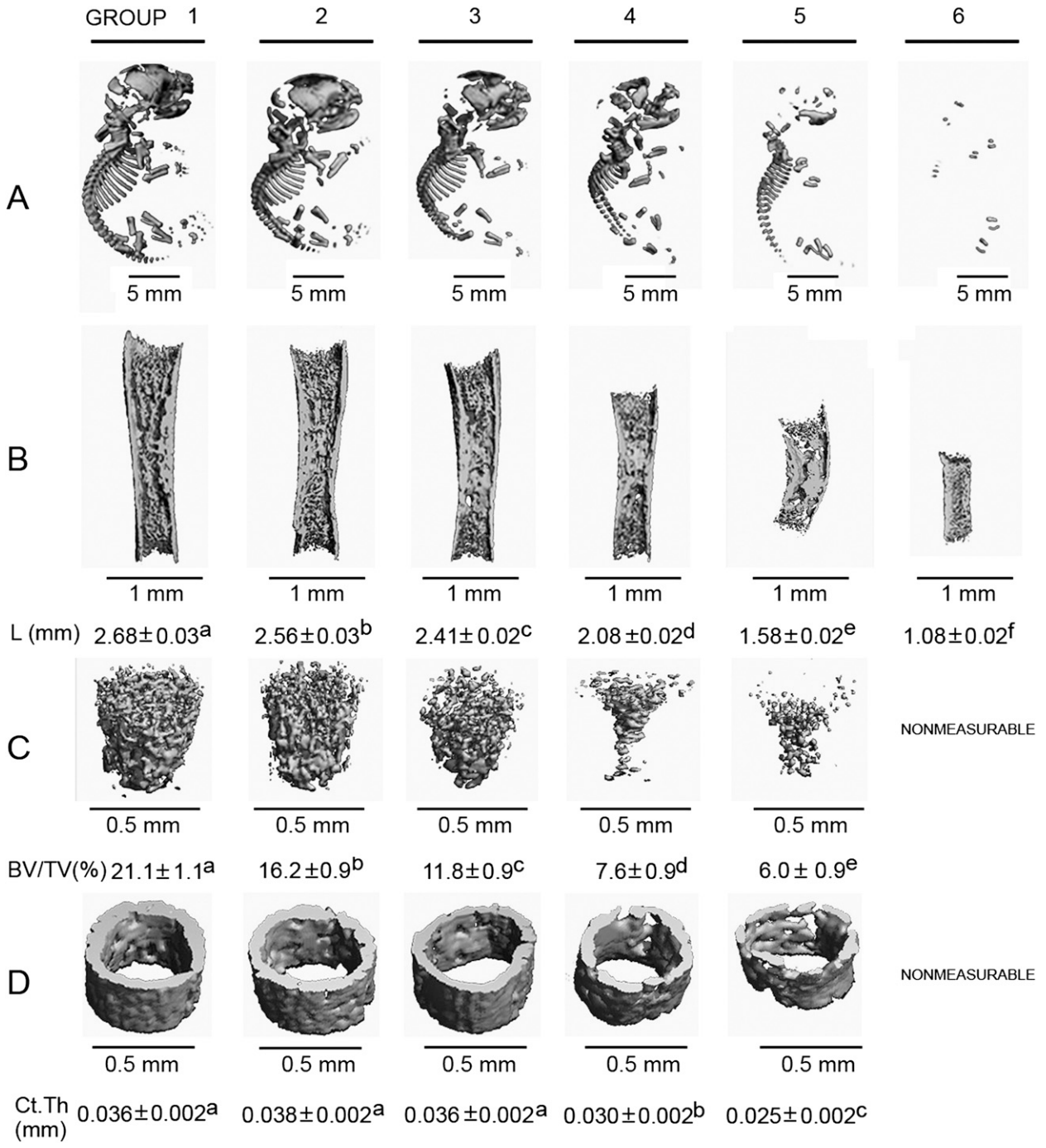

FIG. 4. μCT analysis of compound Runx2-I and -II isoform-deficient newborn mice. Representative 3D images of μCT analysis for the whole skeleton (A), full-length mineralized tibias (B), metaphyseal region (C), and cortical bone (D) of tibias from newborn mice. Compared with the wildtype, there was a gene dose–dependent progression of the severity of the skeletal defects in both endochondral and intramembranous bone (A), decrease in the length of mineralized portion of tibias (B), diminished bone volume (BV/TV%) in metaphyseal bone structures (C), and thinning cortical thickness (Ct.Th) in the cortical bone (D). Data below B, C, and D, respectively, represent the mean ± SD of mineralized tibia length, bone volume, and cortical thickness from four to five mice. Values sharing the same superscript are not significantly different at $p < 0.05$.

newborn mice (Fig. 3). μCT analysis confirmed a more severe reduction in length of mineralized tibia and exhibited tremendous defects in endochondral, intramembranous, and cortical bone formation (Fig. 4). Histological analysis confirmed the marked delay in endochondral ossification in tibias, which only had a narrow bone collar, delay in vascular invasion, and absence of a bone marrow cavity (Fig. 5).

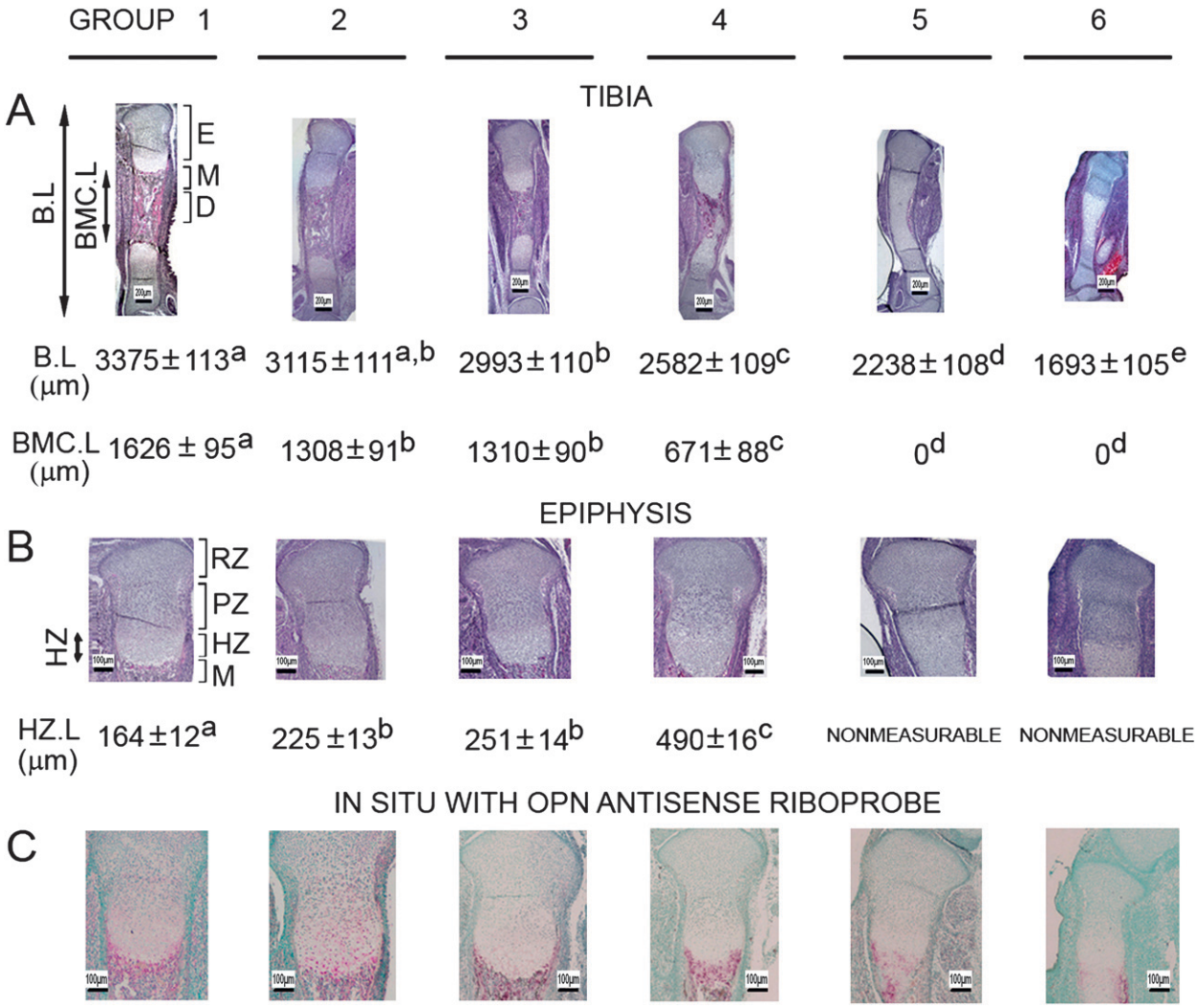

FIG. 5. Histological and in situ analysis of tibial bone in compound *Runx2*-I and -II isoform-deficient E17.5 embryos. (A and B) H&E staining of decalcified tibias. (A) Low magnification (×20) showing epiphyseal and diaphyseal regions. The values below the micrograph represent the bone length (B.L.) and the length of the bone marrow cavity (BMC.L). There was a gene dose–dependent reduction in the length of tibia, formation of bone marrow cavity, and diminished metaphyseal bone formation in the various genotypes. (B) High-power magnification of growth plate (×100). The width of the hypertrophic cartilage zone (HZ) is shown below the micrograph. There is a Runx2 dose-dependent increase in length of hypertrophic zone. E, epiphysis; D, diaphysis; M, metaphysis; B.L, length of tibial bone; BMC.L, length of bone marrow cavity; GP, growth plate; RZ, resting zone; PZ, proliferation zone; HZ, hypertrophic chondrocytes zone; HZ.L, the length of hypertrophic zone. Data are expressed as the mean ± SD from four to five E17.5 embryos, and values sharing the same superscript are not significantly different at $p < 0.05$. (C) Expression of osteopontin by in situ hybridization. Hybridization with *osteopontin* antisense riboprobe was performed. We observed a gene dose–dependent reduction of *osteopontin* (*Opn*) expression (indicated by red staining) in the epiphyseal and diaphyseal regions of tibias from the compound *Runx2* isoform-deficient mice.

Group 6, representing a global deletion of *Runx2*, had the most severe skeletal phenotype, showing the near absence of mineralized bone (Figs. 3–5). However, we did observe rudimentary mineralization in long bones by Alizarin red/Alcian blue skeletal preparations of Runx2-II$^{-/-}$/Runx2-I$^{-/-}$ mice, similar to the reported mineralization of cartilage in these mice.[2,3] μCT analysis also identified some mineralization of the long bone, indicating a small amount of Runx2-independent bone formation. Histological analysis of Runx2-II$^{-/-}$/Runx2-I$^{-/-}$ mice showed the presence of a narrow bone collar but the absence of vascular invasion and bone marrow cavity. In group 6 mice, there was complete absence of the marrow cavity, indicating that the complete loss of Runx2 leads to defects in vascular invasion.[48,49]

Compound selective Runx2-II– and nonselective Runx2–deficient mice show gene dose–dependent effects of Runx2 isoforms on osteoblastic gene expression profiles and osteoblast differentiation.

To study the impact of different amounts of Runx2 on the expression of Runx2-responsive genes in vivo, we next examined the level of osteopontin expression in bone in the

TABLE 2. Gene Expression Profiles in E17.5 Embryos

Gene	Group 2	Group 3	Group 4	Group 5	Group 6	p
Other transcriptional factors						
Runx1	1.25 ± 0.28*	1.69 ± 0.27*	1.47 ± 0.26*	1.56 ± 0.26*	2.85 ± 0.28†	0.0039
Runx3	1.11 ± 0.17*	1.03 ± 0.16*	1.36 ± 0.17*	1.58 ± 0.15†,‡	1.81 ± 0.16‡	0.0246
Cbfβ	0.90 ± 0.10*	0.89 ± 0.09*	0.90 ± 0.09*	0.98 ± 0.10*	0.92 ± 0.09*	0.9125
Msx2	1.04 ± 0.22*	1.59 ± 0.25*,†	1.90 ± 0.28†	2.06 ± 0.29†	3.03 ± 0.29‡	<0.001
Dlx5	1.20 ± 0.24*	1.26 ± 0.23*	1.47 ± 0.24*	1.50 ± 0.24*	2.82 ± 0.25†	<0.001
PPARγ	0.94 ± 0.11*	1.07 ± 0.10*	1.08 ± 0.10*	0.98 ± 0.09*	0.45 ± 0.09†	0.0027
Osteoblast						
Osx	1.05 ± 0.08*	0.63 ± 0.07†	0.66 ± 0.06†	0.33 ± 0.05‡	0.18 ± 0.05‡	<0.001
Bsp	0.62 ± 0.07†	0.35 ± 0.06‡	0.24 ± 0.05‡	0.08 ± 0.02§	0.05 ± 0.01§	<0.001
Akp2	0.97 ± 0.07*	0.69 ± 0.06†	0.51 ± 0.05‡	0.43 ± 0.05‡	0.40 ± 0.04‡	<0.001
Osteocalcin	0.74 ± 0.06*	0.59 ± 0.05†	0.33 ± 0.05‡	0.24 ± 0.04‡,§	0.10 ± 0.04§	<0.001
Osteopontin	0.81 ± 0.08*	0.51 ± 0.07†	0.31 ± 0.06†,‡	0.13 ± 0.05‡,§	0.06 ± 0.05§	<0.001
Collagen I	1.14 ± 0.12*	1.62 ± 0.15†	1.63 ± 0.15†	1.73 ± 0.14†	1.68 ± 0.14†	<0.001
Opg	0.87 ± 0.08*	1.06 ± 0.08*	1.02 ± 0.07*	0.94 ± 0.07*	0.61 ± 0.07†	0.0038
RankL	0.56 ± 0.06†	0.32 ± 0.05‡	0.35 ± 0.05‡	0.22 ± 0.04‡,§	0.17 ± 0.04§	<0.001
Mmp13	0.56 ± 0.07†	0.36 ± 0.06‡	0.15 ± 0.05§	0.08 ± 0.05§	0.02 ± 0.05§	<0.001
Mepe	1.06 ± 0.11*	0.51 ± 0.10†	0.27 ± 0.09†,‡	0.15 ± 0.08‡	0.11 ± 0.08‡	<0.001
Osteocyte						
Dmp1	0.75 ± 0.09*	0.58 ± 0.08*,†	0.32 ± 0.08†,‡	0.20 ± 0.07‡	0.13 ± 0.07‡	<0.001
Phex	0.74 ± 0.08†	0.65 ± 0.08†,‡	0.44 ± 0.07‡,§	0.31 ± 0.07§	0.34 ± 0.07§	<0.001
Osteoclast						
Trap	0.97 ± 0.09*	0.93 ± 0.09*	0.61 ± 0.08†	0.45 ± 0.08†,‡	0.28 ± 0.07‡	<0.001
*Mmp*9	0.95 ± 0.09*	0.61 ± 0.08†	0.40 ± 0.07†,‡	0.26 ± 0.07‡,§	0.15 ± 0.06§	<0.001
Chondrocyte						
VegfA	1.67 ± 0.99*	5.12 ± 1.12†	4.19 ± 0.98†	4.26 ± 0.98†	4.64 ± 0.99†	0.0068
Ihh	1.09 ± 0.09*	1.19 ± 0.08*	0.86 ± 0.08*,†	0.71 ± 0.07†,‡	0.49 ± 0.06‡	<0.001
PthrP	1.06 ± 0.05*	1.48 ± 0.05*	1.44 ± 0.05*	1.41 ± 0.05*	1.98 ± 0.05†	0.007
Collagen X	0.73 ± 0.06†	0.79 ± 0.06†	0.56 ± 0.05‡	0.31 ± 0.05§	0.16 ± 0.05§	<0.001
Sox9	0.87 ± 0.09*	0.81 ± 0.08*	0.85 ± 0.08*	0.90 ± 0.09*	0.91 ± 0.09*	0.7817
Collagen II	0.97 ± 0.12*	1.24 ± 0.11*	1.00 ± 0.11*	1.06 ± 0.12*	1.87 ± 0.13†	0.004

Data are mean ± SD from four to five of E17.5 individual mice and expressed as the fold changes relative to the housekeeping gene *cyclophilin A* and normalized to group 1 wildtype mice.

*, †, ‡, and § indicate a significant difference from group 1 (wildtype), and values sharing the same superscript are not significantly different each other at $p < 0.05$.

Osx, Osterix; Bsp, Bone sialoprotein; *Akp2, Alkaline phosphatase 2; Opg, osteoprotegerin; Phex*, phosphate-regulating gene with homologies to endopeptidases on the X chromosome; *Mepe,* matrix extracellular phosphoglycoprotein; *Dmp1*, dentin matrix protein 1; *VegfA,* vascular endothelial growth factor A; *Trap,* tartrate resistant acid phosphatase; *Mmp*, matrix metalloproteinase. *Ihh*, *Indian hedgehog; PthrP*, parathyroid hormone-like peptide.

different groups by in situ hybridization. O*steopontin,* a Runx2- regulated gene, is mainly expressed in the hypertrophic zone and trabecular bone in the metaphysis in wildtype mice. In addition, *osteopontin* expression in bone was proportionate to the level of *Runx2* expression across the various genotypes (Fig. 5D).

To more widely examine the effect of progressive *Runx2* isoform deficiency on gene expression profiles in bone development, we examined by real-time RT-PCR the expression levels of a panel of osteoblast-, osteoclast-, and chondrocyte-related genes, as well as other transcriptional factors in E17.5 embryos in the various groups (Table 2). We observed a gene dose–dependent reduction of expressed genes in response to the progressive reduction in Runx2 across the various genotypes, including osteoblast/osteocyte-related genes, *Osx*, *Bsp*, *Alk2*, *Oc*, *Op*, *RankL*, *Mmp13*, *Mepe, Dmp1,* and *Phex*; osteoclast-related genes, *Trap* and *Mmp9*; chondrocyte-related genes, *Ihh* and *Col X*; and *PPARγ* (an adipocyte transcription factor). Other genes, including *Vegf*A, *PTHrp*, *Col II*, and *Col I,* as well as the transcription factors *Msx2,* Dlx5, *Runx1,* and *Runx3*, were increased in the presence of Runx2 deficiency, consistent with the presence of compensatory responses to offset the loss of Runx2 and/or sets of genes that are suppressed by *Runx2*. In contrast, progressive Runx2 deficiency across the different genotypes had minimal or no effect on *Cbf*β, *Opg*, and *Sox 9* expression.

Assessment of Runx2 gene dose–dependent effects on osteoblast development ex vivo

To further examine the effect of *Runx2* gene dose on osteoblast development, we characterized the differentiation potential of osteoblast cell lines obtained from the various *Runx2* isoform genotypes. For these ex vivo studies in calvarial-derived osteoblasts, we measured alkaline phosphatase activity, for which the corresponding *Akp2* message showed a Runx2 dose-dependent decrease in whole bone (Table 2) and mineralization of extracellular matrix, a marker of fully differentiated osteoblast function.

TABLE 3. ALP Activity (ηmol/min/μg) in Wildtype and *Runx2*-Deficient Osteoblasts

Genotype	*Group 1*	*Group 2*	*Group 3*	*Group 4*	*Group 5*	*Group 6*
4d	11.8 ± 0.75*	7.9 ± 0.67†	7.8 ± 0.72†	5.0 ± 0.72‡	4.9 ± 0.68‡	3.3 ± 0.54‡
10d	78 ± 3.2*	39 ± 2.5†	35 ± 2.3†	28 ± 1.6‡	22 ± 1.5‡	22 ± 1.8‡
14d	129 ± 5.5*	47 ± 3.6†	43 ± 2.3†	31 ± 2.1‡	27 ± 1.8‡	21 ± 1.2‡

Data are mean ± SD from three triplicates experiments. Values sharing the same footnote symbol are not significantly different each other at $p < 0.05$.

TABLE 4. Calcium Deposition (μmol/well) in Wildtype and *Runx2*-Deficient Osteoblasts

Genotype	*Group 1*	*Group 2*	*Group 3*	*Group 4*	*Greoup 5*	*Group 6*
4d	21.6 ± 2.2*	20.3 ± 2.1*	18.9 ± 1.5*	11.7 ± 1.2†	12.3 ± 1.1†	11.5 ± 1.3†
10d	177 ± 3.7*	148 ± 3.5†	130 ± 3.2‡	95 ± 2.8§	85 ± 2.5§	32 ± 1.6e
14d	715 ± 13*	395 ± 12†	275 ± 11‡	128 ± 9§	84 ± 7e	83 ± 6e

Data are mean ± SD from three triplicates experiments. Values sharing the same footnote symbol are not significantly different each other at $p < 0.05$.

We found that osteoblastic cultures were very sensitive to the loss of Runx2. Indeed, there was a significant reduction in alkaline phosphatase activity and the amount of mineralized extracellular matrix even in osteoblasts derived from group 2 mice that lack only one copy of *Runx2*-II (Tables 3 and 4). Moreover, ex vivo cultures of calvarial-derived osteoblasts from group 3 to group 6 mice showed a progressive reduction in cellular alkaline phosphatase activity and a decrease in the amount of mineralized extracellular matrix compared with group 1 wildtype osteoblasts (Tables 3 and 4), indicating that osteoblast differentiation potential was proportionate to *Runx2* isoform gene dose.

qChIP assay of Runx2-binding to chromatin using an osteocalcin promoter OSE2a site

Finally, we performed quantitative ChIP analyses on immortalized osteoblasts derived from the various genotypes depicted in Fig. 2. Using an anti-Runx2 antibody, we confirmed that Runx2 was specifically recruited to the OSE2a site of the *Osteocalcin* promoter in the differentiated osteoblasts (Fig. 6A). In addition, we observed a 6-fold increase in the ratio of the promoter sequence versus the coding region sequence in the anti-Runx2 group compared with the IgG control group by quantitative real-time PCR from wildtype osteoblasts (Fig. 6B). Consistent with the dose-dependent effects of loss of Runx2 on bone development in vivo, we observed a progressive reduction in Runx2 binding to the *Osteocalcin* promoter from group 1 to group 4. Interestingly, we observed no significant difference between group 4 and group 6, despite intact Runx2-I expression in group 4 and no expression of either Runx2-I or Runx2-II in group 6. This suggests that there may be differential binding of Runx2-I to target promoters or to a threshold effect of Runx2 binding to its target promoters as measured by qChIP analysis (Fig. 6B).

Differential regulation of P1 and P2 promoter of the Runx2 gene

The P1 promoter has been studied, with evidence for Runx2, a vitamin D_3–responsive element, Wnt signaling-responsive TCF (T cell factor)/LEF (lymphoid-enhancer factor) elements, BMP2-responsive homeodomain motifs, AP1, NF1, HLH-related factors, HIF2A, ARNT, ETS-like factors, and SP1 motifs.[39,47,50–52] Little is known about the regulatory elements in the P2 promoter. To support the differential regulation of the P1 and P2 promoters, we used the r*VISTA* promoter analysis program to determine the complement of putative *cis*-acting elements in the respective promoter regions. We identified 130 shared transcription factor binding sites (TFBSs) in the *Runx2* P1 and P2 promoters, 32 unique TFBSs in the 5.4-kb P1 promoter, and 44 unique TFBSs in the 12.0-kb P2 promoter (data not shown). Whereas many of these predicted sites may not represent functional elements, these findings support the likelihood that these promoters are differentially regulated.

To directly assess the response of the two promoters, P1 and P2, promoter-luciferase constructs were transfected into Ros17/2.8 osteoblasts. We found that both Wnt3a and 17β-estradiol (E2) stimulated P1 promoter activity but had no effect on the P2 promoter. In contrast, TGF-β increased P2 promoter activity but suppressed P1 activity. $1,25(OH)_2D_3$ inhibited both P1 and P2 promoter activities in Ros17/2.8 cells (Table 5). We also observed that the activity of the P1 promoter-luciferase construct was ~15-fold greater than the P2 promoter-luciferase construct in both Ros 17/2.8 and MC3T3-E1 osteoblastic cell lines (Fig. 7). In addition, assessment of the transcripts from the P2 and P1 promoters by real-time RT-PCR measurement of their respective unique 5′ UTRs found that the P2-*Runx2*-I 5′-UTR message was upregulated and the P1-*Runx2*-II 5′-UTR was downregulated in E17.5 *Runx2*-null mice (Fig. 7B), suggesting different autoregulation of the two promoters by Runx2. Finally, consistent with the autoregulation of the P1 promoter by Runx2 transcripts,[52] we found that co-transfection of the *Runx2*-II cDNA stimulates P1 but inhibits P2 promoter activity in MC3T3-E1 osteoblasts (Figs. 7C and 7D).

DISCUSSION

The necessity for a complex gene structure of Runx2, with two distinct promoters driving the expression of

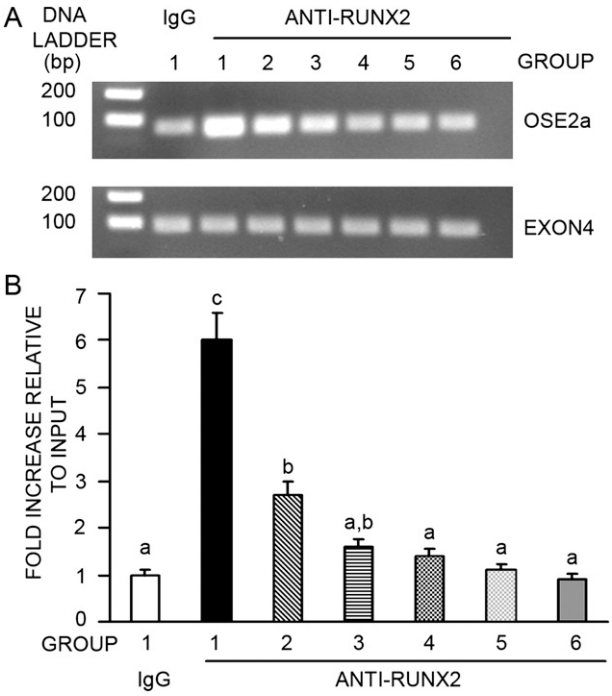

FIG. 6. Analysis of Runx2 binding to the *Osteocalcin* promoter in immortalized calvarial osteoblasts using qChIP assay. (A) Ethidium bromide gel of real-time PCR products obtained with ChIP-DNAs using Runx2 antibody and OSE2a site primers in the *Osteocalcin* promoter. Nonspecific normal rabbit IgG was used as a negative control. (B) Bar graph of the qChIP assay from calvarial osteoblasts. ChIP–DNAs were quantified by real-time PCR using OSE2a site primers in the *Osteocalcin* promoter and exon 4 primers of *Osteocalcin* gene. Values are shown as relative fold of enrichment of the promoter sequence normalized for coding region sequence versus that obtained for input samples and represent the mean ± SD from four independent experiments. Values sharing the same superscript are not significantly different at $p < 0.05$.

TABLE 5. Differential Responses to Stimulation in P1 (1.4 kb) and P2 (2.0 kb) Promoter-Luciferase Reporters in the ROS17/2.8 Osteoblastic Cell Line

Treatment	*Concentration*	*P1 (1.4 kb)*	*P2 (2.0 kb)*
TGF-β	5 ηg/ml	0.71 ± 0.11*	1.75 ± 0.25*
Wnt3A	50% CM	1.51 ± 0.10*	1.03 ± 0.15
17β-estrodal	10^{-7} M	1.50 ± 0.29*	1.04 ± 0.16
1,25$(OH)_2D_3$	10^{-7} M	0.71 ± 0.12*	0.73 ± 0.07*

Relative luciferase activity of P1 or P2 promoter is normalized to the mean ratio of vehicle control, which has been set to and 1. Data are mean ± SD from at least three triplicates experiments.

* Significant difference from vehicle control at $p<0.05$.

similar isoforms that differ only in their N termini, remains uncertain.[27,28,47] In this study, we show that Runx2-I and Runx2-II isoforms exhibit a critical, dose-dependent effect on skeletal development and osteoblast differentiation. Using nonselective *Runx*2 heterozygous mice and selective *Runx*2-II heterozygous mice, we generated mice with graded reductions (~75%, ~50%, and ~25%) in the normal complement of Runx2 protein expression. Phenotypic analysis of mutant mice and isolated osteoblasts showed that progressive reductions in Runx2 levels resulted in proportionate abnormalities in embryonic bone development, expression of osteoblast- and terminal hypertrophic chondrocyte-related genes, and osteoblast development ex vivo. Indeed, Runx2-II$^{+/-}$ (group 2) mice, which retained ~75% of wildtype Runx2 levels, showed a mild defect in skeletogenesis and a significant reduction in a subset of gene transcripts. Interestingly, this reduction is concordant with the decrease to ~70% of wildtype Runx2 required for development of a cleidocranial dysplasia phenotype in mice with a hypomorphic Runx2 mutation.[36]

Runx2-II$^{+/-}$/Runx2-I$^{+/-}$ (group 3) and Runx2-II$^{-/-}$ (group 4) mice, which retained ~50% of the wildtype Runx2 levels, exhibited more severe abnormalities in both endochondral and intramembranous bone formation in association with a greater reduction in a broader range of genes within the osteoblast and chondrocyte lineages. These findings raise questions about the potential differential functions of the Runx2-I and Runx2-II isoforms. In this regard, group 4, which has the loss of the two copies of *Runx2*-II, shows a more severe phenotype than group 3, which has loss of one copy each *Runx2*-II and *Runx2*-I. Because the bone-related *Runx2*-II isoform progressively increases throughout embryonic bone development, whereas the *Runx2*-I isoform is only upregulated in the early skeletal formation[53,54] and both isoforms show similar effects on gene expression,[1,31,34,35,55–60] the greater ''potency'' of the P1 promoter driven product is most likely caused by higher expression during development rather than by unrecognized differential transactivation potential. Studies of selective *Runx2*-I–null mice, however, will be needed to fully address any potential differential function imparted by the distinct N termini of the two isoforms. These mice have been difficult to create because of the inability to achieve homologous recombination over the target region (unpublished observations).

Runx2-II$^{-/-}$/Runx2-I$^{+/-}$ (group 5) mice, which retained ~25% of the normal Runx2 level exclusively from the activity of the P2 promoter and expression of Runx2-I, showed even more severe defects in axial and appendicular bone formation and a significantly greater degree of suppression of osteoblast-related genes. Analysis of group 5, which has only one Runx2-I allele, establishes the minimal requirement of Runx2 for formation of axial and appendicular skeleton, proximal ribs, and mandible. We also showed that the amount of Runx2 isoforms expression correlate with reduction in markers of osteoblast differentiation, as well as Runx2 binding to the osteocalcin promoter by quantitative ChIP analysis in osteoblasts ex vivo. Whereas it has been recognized for some time that there are dose-dependent effects of Runx2 by comparing heterozygous and homozygous Runx2-null mice,[2,3] our studies are the first to establish the dose-dependent effects of Runx2 on bone development in vivo and ex vivo using compound selective *Runx2*-II– and nonselective *Runx2*–deficient mouse models to create a greater range of Runx2 deficiency on the same genetic background.

We also confirmed by in situ hybridization and laser capture RT-PCR that the P2 promoter regulates drives

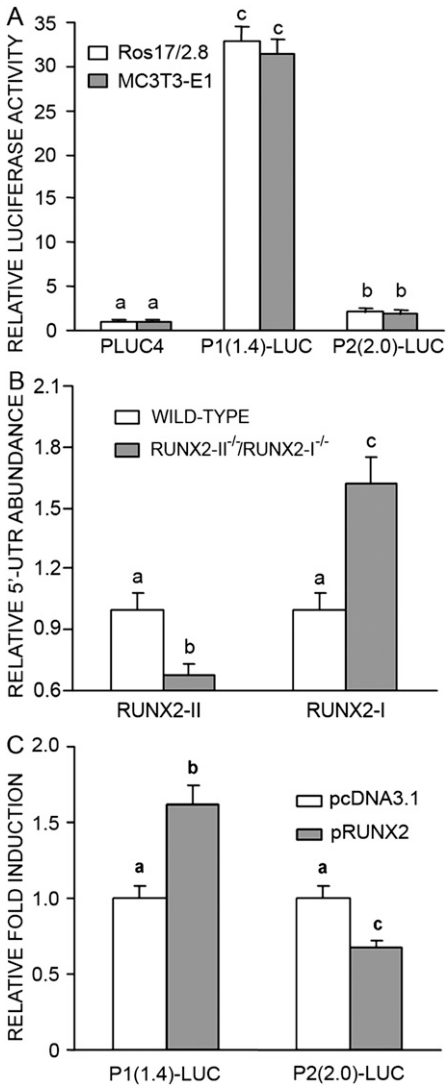

FIG. 7. Autoregulation of *Runx2* P1 and P2 promoter activity by Runx2 isoforms. (A) Relative *Runx2* P1(1.4 kb)-LUC and P2(2.0 kb)-LUC promoter-luciferase reporter activity in Ros17/2.8 and MC3T3-E1 osteoblastic cell lines. (B) 5′-untranslated region (5′-UTR) mRNA levels of *Runx2*-II and *Runx2*-I isoforms in wildtype and Runx2-II$^{-/-}$/Runx2-I$^{-/-}$-null mice were quantified by real-time RT-PCR. Data are mean ± SD from four to five E17.5 individual mice, expressed as the fold changes relative to the housekeeping gene *cyclophilin A,* and normalized to wildtype mice, and values sharing the same superscript are not significantly different each other at $p < 0.05$. (C) Relative *Runx2* P1(1.4 kb)-LUC and P2(2.0 kb)-LUC promoter-luciferase reporter activities were induced by overexpression of *Runx2* using *CMV*-promoter driving *Runx2*-II full-length cDNA plasmid in MC3T3-E1 osteoblasts. Values are shown as relative fold changes to control (pcDNA3.1 vector) and represent the mean ± SD from three independent experiments. Values sharing the same superscript are not significantly different at $p < 0.05$.

*Runx*2-I expression predominately in the perichondrium and periosteum, and to a lesser extent in the proliferating and resting zones of chondrocytes,[61,62] whereas the P1 promoter regulates the expression of *Runx*2-II more widely in the hypertrophic zone, trabecular bone in the metaphysis, and periosteum, but not in the perichondrium.[31,34,63] The site-specific expression of the P1 and P2 promoters may reflect the actions of different signaling pathways on the respective promoters. Indeed, P1 and P2 promoter possess different *cis*-acting elements and are differentially regulated by a variety of factors.[39,58,64–67] Moreover, human SNPs in the *RUNX2* P1 promoter are related to hand bone length,[68,69] whereas human SNPs in the Runx2 P2 promoter are associated with increased BMD, predominately affecting cortical bone.[55,68,70,71] Thus, dual promoter use may permit integration of *Runx2* signaling with environmental enhancers and inhibitors to finely tune the amount of Runx2 and the time and place of *Runx2*-dependent activities during skeletal development and postnatal skeletal homeostasis.

In addition, we showed that Runx2-response genes have different sensitivities to changes in Runx2 transcription factor levels. For example, analysis of E17.5 embryos from group 2 to group 4 mice showed that osteoblastic markers such as *Osterix, Bsp*, *Akp2*, *Osteocalcin*, *Osteopontin*, *RankL, Mmp13,* and *Mepe*,[72–74] osteocyte markers such as *Dmp1* and *Phex*,[75] osteoclast markers such as *Trap* and *Mmp9*,[76] and hypertrophic chondrocyte markers such as *Collagen X*[77] were sensitive to a reduction in Runx2 gene dose. *Bsp*, *Osteocalcin*, *Osteopontin*, *RankL*, *Mmp13*, *Col X*, and *Phex* were the most sensitive to reductions in Runx2, whereas the others were affected only by greater reductions in Runx2. Still other genes were upregulated in a dose-dependent fashion. For example, the arrest of hypertrophic chondrocyte maturation[37,63] correlated with a significant decrement in hypertrophic chondrocytes markers, such as *Type X collagen* and *Ihh*, but increments in *Type II collagen* and *PTHrP*, consistent with impaired terminal chondrogenesis in *Runx2*-deficient mice.[78,79] In addition, increments in *VegfA* in Runx2 deficient mice inversely correlated with the size of the marrow cavity and vascular invasion, suggesting a possible role of Runx2 in the control of angiogenesis.

The mechanism of dose-dependent effects of transcription factors to control gene expression is not well understood. Runx2 dose-dependent effects might be mediated by different affinities for binding to and recruitment of transcriptional co-activators and co-repressors.[14,18,22] A critical threshold concentration of Runx2 proteins may allow co-activators to facilitate activation of osteoblast-specific gene transcription, whereas excessive amounts of Runx2 might sequester co-factors. In this regard, qChIP assays showed a dose-dependent effect of Runx2 binding to *Osteocalcin* promoter with a threshold effect observed with very low levels of Runx2 protein in groups 3 and 4. This latter finding is consistent with the reported decrease in transactional potential of Runx2-I compared with Runx2-II.[15,27,30] In addition, the availability of Runx2 may be influenced by its sequestration. In this regard, sequestration of *Runx2* in the cytoplasm by STAT1 and microtubule dynamics have been shown to inhibit bone development by depleting Runx2 from nuclear microenvironments and may be exacerbated at low levels of Runx2 expression.[20,80] Runx2 might also exert dose-dependent effects through the increased occupancy of additional *cis*-acting binding sites in the promoter of target genes. Increasing amounts of

Runx2 might lead to the recruitment of a greater number of promoters of downstream target genes. In addition, Runx2 may exhibit a dose-dependent effect on lineage-specific control of ribosomal biogenesis through forming complexes with the RNA *Pol*I transcription factors UBF1 and SL1 or through local chromatin histone modification at rDNA regulatory regions.[81,82] Finally, dose-dependent effects of Runx2 might involve epigenetic control of access to *cis*-elements binding sites through interactions with histone deacetylases (HDACs).[22,83,84] In this regard, Runx2 is required for relief of HDAC-mediated repression and enhancement of Runx2 activation of *cis*-acting element promoters in osteoblastic lineages. Further studies will be needed to explore the mechanisms whereby alterations in the amount of Runx2 exerts its transcriptional effects on skeletogenesis.

In conclusion, these studies highlight the importance of Runx2 gene dose and factors modulating P1 and P2 promoter activity in specific subcompartments of bone and at critical times in embryonic development, to ensure the proper skeletal development in mice. A renewed focus on further understanding of the signaling pathways and transactivating factors responsible for the differential control of the P1 and P2 promoters may provide important new insights into environmental factors regulating bone embryogenesis through differential effects to control the time, space, amount, and duration of Runx2 expression through the activities of the P1 and P2 promoters.

ACKNOWLEDGMENTS

This work was supported by the Grant RO1-AR049712 from the National Institutes of Health.

REFERENCES

1. Ducy P, Starbuck M, Priemel M, Shen J, Pinero G, Geoffroy V, Amling M, Karsenty G 1999 A Cbfa1-dependent genetic pathway controls bone formation beyond embryonic development. Genes Dev **13:**1025–1036.
2. Komori T, Yagi H, Nomura S, Yamaguchi A, Sasaki K, Deguchi K, Shimizu Y, Bronson RT, Gao YH, Inada M, Sato M, Okamoto R, Kitamura Y, Yoshiki S, Kishimoto T 1997 Targeted disruption of Cbfa1 results in a complete lack of bone formation owing to maturational arrest of osteoblasts. Cell **89:**755–764.
3. Otto F, Thornell AP, Crompton T, Denzel A, Gilmour KC, Rosewell IR, Stamp GW, Beddington RS, Mundlos S, Olsen BR, Selby PB, Owen MJ 1997 Cbfa1, a candidate gene for cleidocranial dysplasia syndrome, is essential for osteoblast differentiation and bone development. Cell **89:**765–771.
4. Choi JY, Pratap J, Javed A, Zaidi SK, Xing L, Balint E, Dalamangas S, Boyce B, van Wijnen AJ, Lian JB, Stein JL, Jones SN, Stein GS 2001 Subnuclear targeting of Runx/Cbfa/AML factors is essential for tissue-specific differentiation during embryonic development. Proc Natl Acad Sci USA **98:**8650–8655.
5. Vaes BL, Ducy P, Sijbers AM, Hendriks JM, van Someren EP, de Jong NG, van den Heuvel ER, Olijve W, van Zoelen EJ, Dechering KJ 2006 Microarray analysis on Runx2-deficient mouse embryos reveals novel Runx2 functions and target genes during intramembranous and endochondral bone formation. Bone **39:**724–738.
6. Hecht J, Seitz V, Urban M, Wagner F, Robinson PN, Stiege A, Dieterich C, Kornak U, Wilkening U, Brieske N, Zwingman C, Kidess A, Stricker S, Mundlos S 2007 Detection of novel skeletogenesis target genes by comprehensive analysis of a Runx2(−/−) mouse model. Gene Expr Patterns **7:**102–112.
7. Yoshida CA, Furuichi T, Fujita T, Fukuyama R, Kanatani N, Kobayashi S, Satake M, Takada K, Komori T 2002 Core-binding factor beta interacts with Runx2 and is required for skeletal development. Nat Genet **32:**633–638.
8. Xiao ZS, Simpson LG, Quarles LD 2003 IRES-dependent translational control of Cbfa1/Runx2 expression. J Cell Biochem **88:**493–505.
9. Xiao ZS, Thomas R, Hinson TK, Quarles LD 1998 Genomic structure and isoform expression of the mouse, rat and human Cbfa1/Osf2 transcription factor. Gene **214:**187–197.
10. Fujiwara M, Tagashira S, Harada H, Ogawa S, Katsumata T, Nakatsuka M, Komori T, Takada H 1999 Isolation and characterization of the distal promoter region of mouse Cbfa1. Biochim Biophys Acta **1446:**265–272.
11. Aberg T, Wang XP, Kim JH, Yamashiro T, Bei M, Rice R, Ryoo HM, Thesleff I 2004 Runx2 mediates FGF signaling from epithelium to mesenchyme during tooth morphogenesis. Dev Biol **270:**76–93.
12. Ge C, Xiao G, Jiang D, Franceschi RT 2007 Critical role of the extracellular signal-regulated kinase-MAPK pathway in osteoblast differentiation and skeletal development. J Cell Biol **176:**709–718.
13. Stock M, Otto F 2005 Control of RUNX2 isoform expression: The role of promoters and enhancers. J Cell Biochem **95:**506–517.
14. Schroeder TM, Jensen ED, Westendorf JJ 2005 Runx2: A master organizer of gene transcription in developing and maturing osteoblasts. Birth Defects Res C Embryo Today **75:**213–225.
15. Thirunavukkarasu K, Mahajan M, McLarren KW, Stifani S, Karsenty G 1998 Two domains unique to osteoblast-specific transcription factor Osf2/Cbfa1 contribute to its transactivation function and its inability to heterodimerize with Cbfbeta. Mol Cell Biol **18:**4197–4208.
16. Sierra J, Villagra A, Paredes R, Cruzat F, Gutierrez S, Javed A, Arriagada G, Olate J, Imschenetzky M, Van Wijnen AJ, Lian JB, Stein GS, Stein JL, Montecino M 2003 Regulation of the bone-specific osteocalcin gene by p300 requires Runx2/Cbfa1 and the vitamin D3 receptor but not p300 intrinsic histone acetyltransferase activity. Mol Cell Biol **23:**3339–3351.
17. Pelletier N, Champagne N, Stifani S, Yang XJ 2002 MOZ and MORF histone acetyltransferases interact with the Runt-domain transcription factor Runx2. Oncogene **21:**2729–2740.
18. Lian JB, Stein GS, Javed A, van Wijnen AJ, Stein JL, Montecino M, Hassan MQ, Gaur T, Lengner CJ, Young DW 2006 Networks and hubs for the transcriptional control of osteoblastogenesis. Rev Endocr Metab Disord **7:**1–16.
19. Sowa H, Kaji H, Hendy GN, Canaff L, Komori T, Sugimoto T, Chihara K 2004 Menin is required for bone morphogenetic protein 2- and transforming growth factor beta-regulated osteoblastic differentiation through interaction with Smads and Runx2. J Biol Chem **279:**40267–40275.
20. Kim S, Koga T, Isobe M, Kern BE, Yokochi T, Chin YE, Karsenty G, Taniguchi T, Takayanagi H 2003 Stat1 functions as a cytoplasmic attenuator of Runx2 in the transcriptional program of osteoblast differentiation. Genes Dev **17:**1979–1991.
21. Bialek P, Kern B, Yang X, Schrock M, Sosic D, Hong N, Wu H, Yu K, Ornitz DM, Olson EN, Justice MJ, Karsenty G 2004 A twist code determines the onset of osteoblast differentiation. Dev Cell **6:**423–435.
22. Westendorf JJ 2006 Transcriptional co-repressors of Runx2. J Cell Biochem **98:**54–64.
23. Komori T 2005 Regulation of skeletal development by the Runx family of transcription factors. J Cell Biochem **95:**445–453.
24. Komori T 2008 Regulation of bone development and maintenance by Runx2. Front Biosci **13:**898–903.

25. Nimmo R, Woollard A 2008 Worming out the biology of Runx. Dev Biol **313:**492–500.
26. Xiao Z, Awad HA, Liu S, Mahlios J, Zhang S, Guilak F, Mayo MS, Quarles LD 2005 Selective Runx2-II deficiency leads to low-turnover osteopenia in adult mice. Dev Biol **283:**345–356.
27. Xiao ZS, Hjelmeland AB, Quarles LD 2004 Selective deficiency of the ''bone-related'' Runx2-II unexpectedly preserves osteoblast-mediated skeletogenesis. J Biol Chem **279:**20307–20313.
28. Xiao ZS, Hinson TK, Quarles LD 1999 Cbfa1 isoform overexpression upregulates osteocalcin gene expression in non-osteoblastic and pre-osteoblastic cells. J Cell Biochem **74:**596–605.
29. Banerjee C, Javed A, Choi JY, Green J, Rosen V, van Wijnen AJ, Stein JL, Lian JB, Stein GS 2001 Differential regulation of the two principal Runx2/Cbfa1 n-terminal isoforms in response to bone morphogenetic protein-2 during development of the osteoblast phenotype. Endocrinology **142:**4026–4039.
30. Harada H, Tagashira S, Fujiwara M, Ogawa S, Katsumata T, Yamaguchi A, Komori T, Nakatsuka M 1999 Cbfa1 isoforms exert functional differences in osteoblast differentiation. J Biol Chem **274:**6972–6978.
31. Ueta C, Iwamoto M, Kanatani N, Yoshida C, Liu Y, Enomoto-Iwamoto M, Ohmori T, Enomoto H, Nakata K, Takada K, Kurisu K, Komori T 2001 Skeletal malformations caused by overexpression of Cbfa1 or its dominant negative form in chondrocytes. J Cell Biol **153:**87–100.
32. Takeda S, Bonnamy JP, Owen MJ, Ducy P, Karsenty G 2001 Continuous expression of Cbfa1 in nonhypertrophic chondrocytes uncovers its ability to induce hypertrophic chondrocyte differentiation and partially rescues Cbfa1-deficient mice. Genes Dev **15:**467–481.
33. Ji C, Casinghino S, Chang DJ, Chen Y, Javed A, Ito Y, Hiebert SW, Lian JB, Stein GS, McCarthy TL, Centrella M 1998 CBFa(AML/PEBP2)-related elements in the TGF-beta type I receptor promoter and expression with osteoblast differentiation. J Cell Biochem **69:**353–363.
34. Liu W, Toyosawa S, Furuichi T, Kanatani N, Yoshida C, Liu Y, Himeno M, Narai S, Yamaguchi A, Komori T 2001 Overexpression of Cbfa1 in osteoblasts inhibits osteoblast maturation and causes osteopenia with multiple fractures. J Cell Biol **155:**157–166.
35. Geoffroy V, Kneissel M, Fournier B, Boyde A, Matthias P 2002 High bone resorption in adult aging transgenic mice overexpressing cbfa1/runx2 in cells of the osteoblastic lineage. Mol Cell Biol **22:**6222–6233.
36. Lou Y, Javed A, Hussain S, Colby J, Frederick D, Pratap J, Xie R, Gaur T, van Wijnen AJ, Jones SN, Stein GS, Lian JB, Stein JL 2009 A Runx2 threshold for the cleidocranial dysplasia phenotype. Hum Mol Genet **18:**556–568.
37. Enomoto H, Enomoto-Iwamoto M, Iwamoto M, Nomura S, Himeno M, Kitamura Y, Kishimoto T, Komori T 2000 Cbfa1 is a positive regulatory factor in chondrocyte maturation. J Biol Chem **275:**8695–8702.
38. Kwan KM, Pang MK, Zhou S, Cowan SK, Kong RY, Pfordte T, Olsen BR, Sillence DO, Tam PP, Cheah KS 1997 Abnormal compartmentalization of cartilage matrix components in mice lacking collagen X: Implications for function. J Cell Biol **136:**459–471.
39. Xiao Z, Zhang S, Mahlios J, Zhou G, Magenheimer BS, Guo D, Dallas SL, Maser R, Calvet JP, Bonewald L, Quarles LD 2006 Cilia-like structures and polycystin-1 in osteoblasts/osteocytes and associated abnormalities in skeletogenesis and Runx2 expression. J Biol Chem **281:**30884–30895.
40. van der Weyden L, Wei L, Luo J, Yang X, Birk DE, Adams DJ, Bradley A, Chen Q 2006 Functional knockout of the matrilin-3 gene causes premature chondrocyte maturation to hypertrophy and increases bone mineral density and osteoarthritis. Am J Pathol **169:**515–527.
41. Ebraheim NA, Liu J, Shafiq Q, Lu J, Pataparla S, Yeasting RA, Woldenberg L 2006 Quantitative analysis of changes in cervical intervertebral foramen size with vertebral translation. Spine **31:**E62–E65.
42. Borton AJ, Frederick JP, Datto MB, Wang XF, Weinstein RS 2001 The loss of Smad3 results in a lower rate of bone formation and osteopenia through dysregulation of osteoblast differentiation and apoptosis. J Bone Miner Res **16:**1754–1764.
43. Xiao Z, Zhang S, Magenheimer BS, Luo J, Quarles LD 2008 Polycystin-1 regulates skeletogenesis through stimulation of the osteoblast-specific transcription factor RUNX2-II. J Biol Chem **283:**12624–12634.
44. Roca H, Franceschi RT 2008 Analysis of transcription factor interactions in osteoblasts using competitive chromatin immunoprecipitation. Nucleic Acids Res **36:**1723–1730.
45. Loots GG, Ovcharenko I 2004 rVISTA 2.0: Evolutionary analysis of transcription factor binding sites. Nucleic Acids Res **32:**W217–W221.
46. Loots GG, Ovcharenko I, Pachter L, Dubchak I, Rubin EM 2002 rVista for comparative sequence-based discovery of functional transcription factor binding sites. Genome Res **12:**832–839.
47. Xiao ZS, Liu SG, Hinson TK, Quarles LD 2001 Characterization of the upstream mouse Cbfa1/Runx2 promoter. J Cell Biochem **82:**647–659.
48. Pratap J, Lian JB, Javed A, Barnes GL, van Wijnen AJ, Stein JL, Stein GS 2006 Regulatory roles of Runx2 in metastatic tumor and cancer cell interactions with bone. Cancer Metastasis Rev **25:**589–600.
49. Sun L, Vitolo M, Passaniti A 2001 Runt-related gene 2 in endothelial cells: Inducible expression and specific regulation of cell migration and invasion. Cancer Res **61:**4994–5001.
50. Zhang Y, Hassan MQ, Xie RL, Hawse JR, Spelsberg TC, Montecino M, Stein JL, Lian JB, van Wijnen AJ, Stein GS 2009 Co-stimulation of the bone-related Runx2 P1 promoter in mesenchymal cells by SP1 and ETS transcription factors at polymorphic purine-rich DNA sequences (Y-repeats). J Biol Chem **284:**3125–3135.
51. Tamiya H, Ikeda T, Jeong JH, Saito T, Yano F, Jung YK, Ohba S, Kawaguchi H, Chung UI, Choi JY 2008 Analysis of the Runx2 promoter in osseous and non-osseous cells and identification of HIF2A as a potent transcription activator. Gene **416:**53–60.
52. Drissi H, Luc Q, Shakoori R, Chuva De Sousa Lopes S, Choi JY, Terry A, Hu M, Jones S, Neil JC, Lian JB, Stein JL, Van Wijnen AJ, Stein GS 2000 Transcriptional autoregulation of the bone related CBFA1/RUNX2 gene. J Cell Physiol **184:**341–350.
53. Smith N, Dong Y, Lian JB, Pratap J, Kingsley PD, van Wijnen AJ, Stein JL, Schwarz EM, O'Keefe RJ, Stein GS, Drissi MH 2005 Overlapping expression of Runx1(Cbfa2) and Runx2(Cbfa1) transcription factors supports cooperative induction of skeletal development. J Cell Physiol **203:**133–143.
54. Wang Y, Belflower RM, Dong YF, Schwarz EM, O'Keefe RJ, Drissi H 2005 Runx1/AML1/Cbfa2 mediates onset of mesenchymal cell differentiation toward chondrogenesis. J Bone Miner Res **20:**1624–1636.
55. Doecke JD, Day CJ, Stephens AS, Carter SL, van Daal A, Kotowicz MA, Nicholson GC, Morrison NA 2006 Association of functionally different RUNX2 P2 promoter alleles with BMD. J Bone Miner Res **21:**265–273.
56. Jones DC, Wein MN, Oukka M, Hofstaetter JG, Glimcher MJ, Glimcher LH 2006 Regulation of adult bone mass by the zinc finger adapter protein Schnurri-3. Science **312:**1223–1227.
57. Selvamurugan N, Jefcoat SC, Kwok S, Kowalewski R, Tamasi JA, Partridge NC 2006 Overexpression of Runx2 directed by the matrix metalloproteinase-13 promoter containing the AP-1 and Runx/RD/Cbfa sites alters bone remodeling in vivo. J Cell Biochem **99:**545–557.
58. Hassan MQ, Tare RS, Lee SH, Mandeville M, Morasso MI, Javed A, van Wijnen AJ, Stein JL, Stein GS, Lian JB 2006 BMP2 commitment to the osteogenic lineage involves activation of Runx2 by DLX3 and a homeodomain transcriptional network. J Biol Chem **281:**40515–40526.
59. Kanatani N, Fujita T, Fukuyama R, Liu W, Yoshida CA, Moriishi T, Yamana K, Miyazaki T, Toyosawa S, Komori T 2006 Cbf beta regulates Runx2 function isoform-dependently in postnatal bone development. Dev Biol **296:**48–61.

60. Nakashima K, Zhou X, Kunkel G, Zhang Z, Deng JM, Behringer RR, de Crombrugghe B 2002 The novel zinc finger-containing transcription factor osterix is required for osteoblast differentiation and bone formation. Cell **108:**17–29.
61. Choi KY, Lee SW, Park MH, Bae YC, Shin HI, Nam S, Kim YJ, Kim HJ, Ryoo HM 2002 Spatio-temporal expression patterns of Runx2 isoforms in early skeletogenesis. Exp Mol Med **34:**426–433.
62. Park MH, Shin HI, Choi JY, Nam SH, Kim YJ, Kim HJ, Ryoo HM 2001 Differential expression patterns of Runx2 isoforms in cranial suture morphogenesis. J Bone Miner Res **16:**885–892.
63. Inada M, Yasui T, Nomura S, Miyake S, Deguchi K, Himeno M, Sato M, Yamagiwa H, Kimura T, Yasui N, Ochi T, Endo N, Kitamura Y, Kishimoto T, Komori T 1999 Maturational disturbance of chondrocytes in Cbfa1-deficient mice. Dev Dyn **214:**279–290.
64. Gaur T, Lengner CJ, Hovhannisyan H, Bhat RA, Bodine PV, Komm BS, Javed A, van Wijnen AJ, Stein JL, Stein GS, Lian JB 2005 Canonical WNT signaling promotes osteogenesis by directly stimulating Runx2 gene expression. J Biol Chem **280:**33132–33140.
65. Lee MH, Kim YJ, Kim HJ, Park HD, Kang AR, Kyung HM, Sung JH, Wozney JM, Kim HJ, Ryoo HM 2003 BMP-2-induced Runx2 expression is mediated by Dlx5, and TGF-beta 1 opposes the BMP-2-induced osteoblast differentiation by suppression of Dlx5 expression. J Biol Chem **278:**34387–34394.
66. Pan W, Quarles LD, Song LH, Yu YH, Jiao C, Tang HB, Jiang CH, Deng HW, Li YJ, Zhou HH, Xiao ZS 2005 Genistein stimulates the osteoblastic differentiation via NO/cGMP in bone marrow culture. J Cell Biochem **94:**307–316.
67. Gilbert L, He X, Farmer P, Rubin J, Drissi H, van Wijnen AJ, Lian JB, Stein GS, Nanes MS 2002 Expression of the osteoblast differentiation factor RUNX2 (Cbfa1/AML3/Pebp2alpha A) is inhibited by tumor necrosis factor-alpha. J Biol Chem **277:**2695–2701.
68. Ermakov S, Malkin I, Keter M, Kobyliansky E, Livshits G 2008 Family-based association study of polymorphisms in the RUNX2 locus with hand bone length and hand BMD. Ann Hum Genet **72:**510–518.
69. Ermakov S, Malkin I, Kobyliansky E, Livshits G 2006 Variation in femoral length is associated with polymorphisms in RUNX2 gene. Bone **38:**199–205.
70. Napierala D, Garcia-Rojas X, Sam K, Wakui K, Chen C, Mendoza-Londono R, Zhou G, Zheng Q, Lee B 2005 Mutations and promoter SNPs in RUNX2, a transcriptional regulator of bone formation. Mol Genet Metab **86:**257–268.
71. Bustamante M, Nogues X, Agueda L, Jurado S, Wesselius A, Caceres E, Carreras R, Ciria M, Mellibovsky L, Balcells S, Diez-Perez A, Grinberg D 2007 Promoter 2 -1025 T/C polymorphism in the RUNX2 gene is associated with femoral neck bmd in Spanish postmenopausal women. Calcif Tissue Int **81:**327–332.
72. Nishio Y, Dong Y, Paris M, O'Keefe RJ, Schwarz EM, Drissi H 2006 Runx2-mediated regulation of the zinc finger Osterix/Sp7 gene. Gene **372:**62–70.
73. Jimenez MJ, Balbin M, Lopez JM, Alvarez J, Komori T, Lopez-Otin C 1999 Collagenase 3 is a target of Cbfa1, a transcription factor of the runt gene family involved in bone formation. Mol Cell Biol **19:**4431–4442.
74. Roca H, Franceschi RT 2008 Analysis of transcription factor interactions in osteoblasts using competitive chromatin immunoprecipitation. Nucleic Acids Res **36:**1723–1730.
75. Fen JQ, Zhang J, Dallas SL, Lu Y, Chen S, Tan X, Owen M, Harris SE, MacDougall M 2002 Dentin matrix protein 1, a target molecule for Cbfa1 in bone, is a unique bone marker gene. J Bone Miner Res **17:**1822–1831.
76. Pratap J, Javed A, Languino LR, van Wijnen AJ, Stein JL, Stein GS, Lian JB 2005 The Runx2 osteogenic transcription factor regulates matrix metalloproteinase 9 in bone metastatic cancer cells and controls cell invasion. Mol Cell Biol **25:**8581–8591.
77. Zheng Q, Zhou G, Morello R, Chen Y, Garcia-Rojas X, Lee B 2003 Type X collagen gene regulation by Runx2 contributes directly to its hypertrophic chondrocyte-specific expression in vivo. J Cell Biol **162:**833–842.
78. Hinoi E, Bialek P, Chen YT, Rached MT, Groner Y, Behringer RR, Ornitz DM, Karsenty G 2006 Runx2 inhibits chondrocyte proliferation and hypertrophy through its expression in the perichondrium. Genes Dev **20:**2937–2942.
79. Liu Z, Lavine KJ, Hung IH, Ornitz DM 2007 FGF18 is required for early chondrocyte proliferation, hypertrophy and vascular invasion of the growth plate. Dev Biol **302:**80–91.
80. Pockwinse SM, Rajgopal A, Young DW, Mujeeb KA, Nickerson J, Javed A, Redick S, Lian JB, van Wijnen AJ, Stein JL, Stein GS, Doxsey SJ 2006 Microtubule-dependent nuclear-cytoplasmic shuttling of Runx2. J Cell Physiol **206:**354–362.
81. Young DW, Hassan MQ, Pratap J, Galindo M, Zaidi SK, Lee SH, Yang X, Xie R, Javed A, Underwood JM, Furcinitti P, Imbalzano AN, Penman S, Nickerson JA, Montecino MA, Lian JB, Stein JL, van Wijnen AJ, Stein GS 2007 Mitotic occupancy and lineage-specific transcriptional control of rRNA genes by Runx2. Nature **445:**442–446.
82. Young DW, Hassan MQ, Yang XQ, Galindo M, Javed A, Zaidi SK, Furcinitti P, Lapointe D, Montecino M, Lian JB, Stein JL, van Wijnen AJ, Stein GS 2007 Mitotic retention of gene expression patterns by the cell fate-determining transcription factor Runx2. Proc Natl Acad Sci USA **104:**3189–3194.
83. Jensen ED, Nair AK, Westendorf JJ 2007 Histone deacetylase co-repressor complex control of Runx2 and bone formation. Crit Rev Eukaryot Gene Expr **17:**187–196.
84. Schroeder TM, Westendorf JJ 2005 Histone deacetylase inhibitors promote osteoblast maturation. J Bone Miner Res **20:**2254–2263.
85. Sun L, Vitolo MI, Qiao M, Anglin IE, Passaniti A 2004 Regulation of TGFbeta1-mediated growth inhibition and apoptosis by RUNX2 isoforms in endothelial cells. Oncogene **23:**4722–4734.

Received in original form October 14, 2008; revised form February 18, 2009; accepted May 1, 2009.